Chinese Journal of Aeronautics, (2014),27(4): 835–845

Chinese Society of Aeronautics and Astronautics
& Beihang University

Chinese Journal of Aeronautics

cja@buaa.edu.cn
www.sciencedirect.com

Correlation analysis of PCB and comparison of test-analysis model reduction methods

Xu Fei, Li Chuanri *, Jiang Tongmin, Rong Shuanglong

School of Reliability and Systems Engineering, Beihang University, Beijing 100191, China

Received 13 July 2013; revised 27 March 2014; accepted 14 April 2014
Available online 5 July 2014

KEYWORDS

Correlation analysis;
Excitation and measurement point;
Finite element method;
Modal analysis;
Model reduction;
PCB

Abstract The validity of correlation analysis between finite element model (FEM) and modal test data is strongly affected by three factors, i.e., quality of excitation and measurement points in modal test, FEM reduction methods, and correlation check techniques. A new criterion based on modified mode participation (MMP) for choosing the best excitation point is presented. Comparison between this new criterion and mode participation (MP) criterion is made by using Case 1 with a simple printed circuit board (PCB). The result indicates that this new criterion produces better results. In Case 2, 35 measurement points are selected to perform modal test and correlation analysis while 9 selected in Case 3. System equivalent reduction expansion process (SEREP), modal assurance criteria (MAC), coordinate modal assurance criteria (CoMAC), pseudo orthogonality check (POC) and coordinate orthogonality check (CORTHOG) are used to show the error introduced by modal test in Cases 2 and 3. Case 2 shows that additional errors which cannot be identified by using CoMAC can be found by using CORTHOG. In both Cases 2 and 3, Guyan reduction, improved reduced system (IRS) method, SEREP and Hybrid reduction are compared for accuracy and robustness. The results suggest that the quality of the reduction process is problem dependent. However, the IRS method is an improvement over the Guyan reduction, and the Hybrid reduction is an improvement over the SEREP reduction.

1. Introduction

Finite element model (FEM) is widely used to study the dynamic characteristics of printed circuit board (PCB) nowadays.[1–6] FEM needs to be validated by modal test data to ensure its accuracy. When good correlation between test data and FEM is obtained, the FEM is considered to be acceptable. Otherwise, either FEM needs to be updated or test data needs to be improved. Since there are usually some uncertain parameters and inaccurate assumptions in FEM, i.e., uncertainty of geometrical and material parameters, discretization of structures and inaccurate assumption of boundary conditions, results from FEM are usually considered to be less accurate relative to modal test data. However, errors can also arise as a result of inappropriate selection of excitation and measurement points in modal test, mass effect of a roving accelerometer, aliasing, spectral leakage, linearization of non-linear effects and modal parameter extraction, etc.

* Corresponding author. Tel.: +86 10 82339683.
E-mail addresses: daniel_srse_buaa@dse.buaa.edu.cn (F. Xu), lichuanri@buaa.edu.cn (C. Li).

Peer review under responsibility of Editorial Committee of CJA.

Production and hosting by Elsevier

http://dx.doi.org/10.1016/j.cja.2014.06.008

Among these errors introduced in modal test, the problem of sensor placement can be investigated by several approaches.[7–9] Mode participation is a basic tool to be used to evaluate the effectiveness of each excitation points for all selected modes and to select the best excitation point.[10]

Natural frequencies from modal test can be compared with FEM results directly, but mode shapes cannot. In general, the FEM will have more degree of freedom (DOFs) than that used in the test configuration. In order to compare the FEM mode shapes with the test results directly, one way is to produce a reduced representation or test-analysis model (TAM) by using model reduction methods. The DOFs of the TAM will correspond to measurement points in the modal test configuration. Model reduction method can be classified into approximation and exact methods. Guyan has presented a static reduction method, which only considered the static equilibrium in structures.[11] This is the method used in most FE software. Improved reduced system (IRS) has been presented by O'Callahan.[12] This process uses Guyan reduction as an estimate of the reduced system and then makes adjustments to compensate for the inertia effects which are ignored in the Guyan process. IRS is supposed to produce more accurate prediction of the system dynamics. These two methods mentioned above are referred to as approximation methods. The advantage of approximation methods is that they can perform the eigensolution quickly and effectively. The disadvantage is that the application of this kind of method depends largely on the number and location of DOFs. Inappropriate selection of DOFs may introduce large errors. SEREP has been shown to exactly map the mass and stiffness matrices for a desired set of modes at an arbitrary set of DOFs.[13] These reduced matrices will exactly represent the actual dynamics of the full model for the selected set of modes. However, these reduced matrices can only be formulated if an eigensolution of the full system is available. It has been observed that in some cases the use of a system equivalent reduction expansion process (SEREP) TAM in orthogonality check (ORTHOG) computations can result in larger off-diagonal terms than the corresponding values produced by a less accurate static TAM, which means that the robustness of SEREP needs to be considered when it is used. Sairajan used a probabilistic approach to assess the robustness of a SEREP based TAM when experimental and analytical modes contain different levels of inaccuracy.[14] Kammer has extended the capabilities of the SEREP method and presented the Hybrid method.[15] This method combines the accuracy of SEREP with the robustness of the Guyan reduction. Nimityongskul has presented a new model reduction method based on frequency response function (FRF).[16] Koutsovasilis compares some of the model reduction techniques for elastic piston rod. The validity of the reduced models is checked by applying modal correlation criteria.[17]

Correlation analysis can be classified into vector correlation and DOF correlation. Vector correlation provides a global indicator of the level of agreement achieved, and DOF correlation provides an indicator as to how individual DOFs contribute to the overall modal vector correlation.

Modal assurance criteria (MAC) is the earliest presented and most commonly used modal-based correlation check technique. One advantage of MAC is that it is independent of any weighting functions. Another level of vector correlation commonly employed involves an ORTHOG with the system mass matrix.

In the same manner in which the vectors are checked for correlation, the individual vector DOFs can also be checked. One technique based on MAC is the coordinate modal assurance criteria (CoMAC) which helps to identify the contribution of individual DOFs to the MAC and identify areas of the structure which may contain discrepancy. If the system mass matrix is included in these computations, then a formulation referred to as the coordinate orthogonality check (CORTHOG) can be developed which identifies how each individual DOF contributes to the pseudo orthogonality check (POC) terms on a mass scaled basis; the CORTHOG allows for more critical evaluation of DOF correlation since mass matrix is included in this correlation.

All correlation techniques mentioned above is modal-based. Some authors presented FRF-based correlation techniques.[18–20] These techniques compare the FRF directly without any modal analysis. Refs.[21–23] reviewed some of these correlation techniques mentioned above.

This paper presents a new criterion to choose the best excitation point in a hammer-used modal test. Theory behind some reduction methods and correlation check techniques is reviewed. Errors introduced by inappropriate selection of measurement points and poor measured test data are identified. Guyan reduction, IRS method, SEREP and Hybrid reduction are compared for accuracy and robustness.

2. Theory

The theoretical aspects can be broken up into several parts consisting of the deviation of the formulation of the modified mode participation (MMP), the general formulation of the correlation check techniques (MAC, CoMAC, ORTHOG and CORTHOG) and the model reduction methods (Guyan reduction, IRS, SEREP and Hybrid reduction).

2.1. Modified mode participation

The new criterion is based on MMP. The original MP can be used to evaluate the effectiveness of each excitation points for all selected modes [4] and formulated as

$$\mathrm{MP}_{qi} = \sum_{p=1}^{N_\mathrm{o}} |R_{pqi}| \quad (q = 1, 2, \ldots, N_\mathrm{i}; \quad i = 1, 2, \ldots, N_\mathrm{m}) \tag{1}$$

where p denotes the output DOF, q the input DOF, i the mode number; N_o the number of output DOF, N_i the number of input DOF, N_m the number of modes, and R_{pqi} the residue.

High value of MP_{qi} indicates high effectiveness of qth excitation point for ith mode. If the MP_{qi} is simply summed for all selected modes, the MP_q can be used to evaluate the effectiveness of qth excitation point for those modes.

$$\mathrm{MP}_q = \sum_{i=1}^{N_\mathrm{m}} \mathrm{MP}_{qi} \quad (q = 1, 2, \ldots, N_\mathrm{i}) \tag{2}$$

For a general multi-degree-of-freedom (MDOF) system, the transfer function (TF) between excitation point q and response point p can be written as

$$H_{pq}(S) = \sum_{i=1}^{N_\mathrm{m}} \frac{R_{pqi}}{S - P_i} + \frac{R^*_{pqi}}{S - P^*_i} \tag{3}$$

$$R_{pqi} = \frac{\phi_{pi}\phi_{qi}}{j2\omega_{ni}\sqrt{1-\xi_i^2}} \tag{4}$$

where S denotes the Laplace variable, j the imaginary unit, P_i the ith pole, ϕ_{pi}, ϕ_{qi} denote (i, p) and (i, q) term respectively in modal matrix which is normalized with respect to mass matrix, ω_{ni} denotes ith natural frequency in rad/s, and ξ_i denotes ith modal damping ratio (zero for undamped system). Then Eq. (1) can be written as

$$\begin{aligned} \mathrm{MP}_{qi} = \sum_{p=1}^{N_o}|R_{pqi}| &= \sum_{p=1}^{N_o}\left|\frac{\phi_{pi}\phi_{qi}}{j2\omega_{ni}\sqrt{1-\xi_i^2}}\right| \\ &= |\phi_{qi}|\sum_{p=1}^{N_o}\left|\frac{\phi_{pi}}{j2\omega_{ni}\sqrt{1-\xi_i^2}}\right| \\ &(q = 1, 2, \ldots, N_i; \quad i = 1, 2, \ldots, N_m) \end{aligned} \tag{5}$$

For the ith mode, $\sum_{p=1}^{N_o}\left|\frac{\phi_{pi}}{j2\omega_{ni}\sqrt{1-\xi_i^2}}\right|$ is the same for all excitation points. Thus, $|\phi_{qi}|$ can be used to evaluate the effectiveness of qth excitation point for selected mode. Here we use ϕ_{qi}^2 instead of $|\phi_{qi}|$ to make the comparison between different excitation points more clearly. The MMP can be written as

$$\mathrm{MMP}_{qi} = \phi_{qi}^2 \quad (q = 1, 2, \ldots, N_i; \quad i = 1, 2, \ldots, N_m) \tag{6}$$

Then Eq. (2) can be written as

$$\mathrm{MMP}_q = \sum_{i=1}^{N_m}\mathrm{MMP}_{qi} \quad (q = 1, 2, \ldots, N_i) \tag{7}$$

Then MMP_q can be used to evaluate the effectiveness of qth excitation point for those selected modes and produce the same results as MP criterion. Criterion based on MMP_q is referred as the old criterion. A problem with this criterion is that the value of MMP_q may be high but the value of one or more MMP_{qi} may be low themselves (even zero). This indicates that high value of MMP_q does not mean high effectiveness of qth excitation point for each selected mode. To find a way to overcome this problem, a new criterion based on maximizing the "smallest" resonance is presented. For all the selected modes, each excitation point has a minimum MMP_{qi}. Excitation point which has the largest value of minimum MMP_{qi} is considered to be the best point in single input modal test. In this case, all selected modes can be excited. Comparison between these two criteria is made by using Case 1.

2.2. Correlation check techniques

2.2.1. MAC

The modal assurance criteria is a commonly used method for assessing the degree of correlation between any two (i.e., analytical and experimental) vectors and is formulated as

$$\mathrm{MAC}_{ij} = \frac{(\boldsymbol{u}_i^{\mathrm{T}}\boldsymbol{e}_j)^2}{(\boldsymbol{u}_i^{\mathrm{T}}\boldsymbol{u}_i)(\boldsymbol{e}_j^{\mathrm{T}}\boldsymbol{e}_j)} \tag{8}$$

where $\boldsymbol{u}_i$ denotes the ith vector from analytical modal matrix, and $\boldsymbol{e}_j$ the jth vector from experimental modal matrix.

With values ranging from 0 to 1, low values of MAC indicate very little correlation between the two vectors and high values indicate very high correlation. However, there can be situations, e.g., not enough measurement points in the modal test, where MAC will show correlation between vectors which are actually independent.

2.2.2. Orthogonality check

To overcome some of these limitations of MAC, many times an orthogonality check between the experimental vectors or between the experimental and analytical vectors using an analytical mass matrix is attempted:

$$\mathrm{ORTHOG} = \boldsymbol{E}^{\mathrm{T}}\boldsymbol{M}\boldsymbol{E} \tag{9}$$

$$\mathrm{POC} = \boldsymbol{E}^{\mathrm{T}}\boldsymbol{M}\boldsymbol{U} \tag{10}$$

where $\boldsymbol{E}$ denotes the experimental modal matrix, $\boldsymbol{M}$ the mass matrix, $\boldsymbol{U}$ the analytical modal matrix.

The orthogonality check and pseudo orthogonality check can be performed by checking if ORTHOG and POC equal identity matrix $\boldsymbol{I}$ respectively.

This can be done at either tested DOF or full finite element DOF. Typically, the closer the POC off-diagonal terms are to zero, the better correlation between the analytical and experimental modal vectors.

2.2.3. CoMAC

The coordinate modal assurance criteria is an indication of the contribution of each degree of freedom to the MAC values for a given pair and is formulated as

$$\mathrm{CoMAC}(p) = \frac{\left[\sum_{i=1}^{N_m}\left|\boldsymbol{u}_p^i\boldsymbol{e}_p^i\right|\right]^2}{\sum_{i=1}^{N_m}(\boldsymbol{u}_p^i)^2\sum_{i=1}^{N_m}(\boldsymbol{e}_p^i)^2} \tag{11}$$

where $\boldsymbol{u}_p^i$ denotes pth element of ith vector from analytical modal matrix, $\boldsymbol{e}_p^i$ denotes pth element of ith vector from experimental modal matrix.

With values ranging from 0 to 1, low values of CoMAC indicate very little correlation between the two vectors and high values indicate very high correlation.

2.2.4. CORTHOG

Each term of the POC matrix can be described in index notation as

$$\mathrm{POC}_{ij} = \sum_p\sum_q e_{pi}m_{pq}u_{qj} \tag{12}$$

where e_{pi} denotes the pth element of ith vector from experimental modal matrix, m_{pq} the (p, q) element of mass matrix, u_{qj} the qth element of jth vector from analytical modal matrix.

A problem is that the individual multiplications that make up one POC off-diagonal term can be inspected, but there is no way to assess whether a given value is too high or too low if just "emu" is evaluated. An approach is to normalize the computed difference to the maximum difference given as

$$\mathrm{CORTHOG}_{ij}^{pq} = \frac{e_{pi}m_{pq}u_{qj} - u_{pi}m_{pq}u_{qj}}{\sum_{p=1}^{n}\sum_{q=1}^{n}(e_{pi}m_{pq}u_{qj} - u_{pi}m_{pq}u_{qj})} \tag{13}$$

which is referred to as the CORTHOG. This check is written for each DOF pair (p, q) and for each mode pair (i, j) that is investigated.

2.3. Model reduction methods

All of the model reduction methods are based on transformation methods of the form[16]:

$$\boldsymbol{B} = \boldsymbol{T}_{\text{trans}}^{\text{T}} \boldsymbol{A} \boldsymbol{T}_{\text{trans}} \tag{14}$$

where $\boldsymbol{A}$ denotes the original matrix, $\boldsymbol{B}$ the new matrix, and $\boldsymbol{T}_{\text{trans}}$ the transformation matrix.

The key difference between each reduction method is the transformation matrix $\boldsymbol{T}_{\text{trans}}$. The accuracy and robustness of each method is determined by the information used to construct the transformation matrix.

2.3.1. Guyan reduction

The simplest TAM procedure uses the Guyan reduction method. This method is based on solving a static problem:

$$\begin{bmatrix} \boldsymbol{F}_{\text{a}} \\ \boldsymbol{F}_{\text{d}} \end{bmatrix} = \begin{bmatrix} \boldsymbol{K}_{\text{aa}} & \boldsymbol{K}_{\text{ad}} \\ \boldsymbol{K}_{\text{da}} & \boldsymbol{K}_{\text{dd}} \end{bmatrix} \begin{bmatrix} \boldsymbol{X}_{\text{a}} \\ \boldsymbol{X}_{\text{d}} \end{bmatrix} \tag{15}$$

where $\boldsymbol{F}_{\text{a}}$ denotes the active DOF force vector, $\boldsymbol{F}_{\text{d}}$ the deleted DOF force vector, $\boldsymbol{X}_{\text{a}}$ the active DOF displacement vector, $\boldsymbol{X}_{\text{d}}$ the deleted DOF displacement vector, $\boldsymbol{K}_{ij} (i = \text{a, d}; j = \text{a, d})$ the partitioned stiffness matrices.

The transformation matrix $\boldsymbol{T}_{\text{static}}$ from the FEM DOF to the TAM DOF is

$$\boldsymbol{T}_{\text{static}} = \begin{bmatrix} \boldsymbol{I} \\ -\boldsymbol{K}_{\text{dd}}^{-1} \boldsymbol{K}_{\text{da}} \end{bmatrix} \tag{16}$$

The reduced mass and stiffness matrices can now be formed using the original FEM matrices and the transformation matrix:

$$\boldsymbol{M}_{\text{a}} = \boldsymbol{T}_{\text{static}}^{\text{T}} \boldsymbol{M}_n \boldsymbol{T}_{\text{static}} \tag{17}$$

$$\boldsymbol{K}_{\text{a}} = \boldsymbol{T}_{\text{static}}^{\text{T}} \boldsymbol{K}_n \boldsymbol{T}_{\text{static}} \tag{18}$$

where $\boldsymbol{M}_{\text{a}}$ denotes the reduced mass matrix, $\boldsymbol{M}_n$ the original FEM mass matrix, $\boldsymbol{K}_{\text{a}}$ the reduced stiffness matrix, $\boldsymbol{K}_n$ the original FEM stiffness matrix.

2.3.2. IRS

This method improves upon the Guyan reduction by including mass effects in the development of the transformation matrix. The final transformation matrix for the IRS method is

$$\boldsymbol{T}_{\text{IRS}} = \boldsymbol{T}_{\text{static}} + \boldsymbol{T}_{\text{dynamic}} \tag{19}$$

where

$$\boldsymbol{T}_{\text{dynamic}} = \boldsymbol{S} \boldsymbol{M}_n \boldsymbol{T}_{\text{static}} \boldsymbol{M}_{\text{a\_Guyan}}^{-1} \boldsymbol{K}_{\text{a\_Guyan}} \tag{20}$$

where $\boldsymbol{M}_{\text{a\_Guyan}}$ denotes reduced mass matrix in Guyan reduction, and $\boldsymbol{K}_{\text{a\_Guyan}}$ reduced stiffness matrix in Guyan reduction.

$$\boldsymbol{S} = \begin{bmatrix} \boldsymbol{0} & \boldsymbol{0} \\ \boldsymbol{0} & \boldsymbol{K}_{\text{dd}}^{-1} \end{bmatrix} \tag{21}$$

The reduced mass and stiffness matrices can be written as

$$\boldsymbol{M}_{\text{a}} = \boldsymbol{T}_{\text{IRS}}^{\text{T}} \boldsymbol{M}_n \boldsymbol{T}_{\text{IRS}} \tag{22}$$

$$\boldsymbol{K}_{\text{a}} = \boldsymbol{T}_{\text{IRS}}^{\text{T}} \boldsymbol{K}_n \boldsymbol{T}_{\text{IRS}} \tag{23}$$

2.3.3. SEREP

The mapping transformation matrix for SEREP method can be written as

$$\boldsymbol{T}_{\text{SEREP}} = \boldsymbol{\Phi}_n \boldsymbol{\Phi}_{\text{a}}^{\text{g}} \tag{24}$$

where $\boldsymbol{\Phi}_n$ is referred to as the modal matrix, $\boldsymbol{\Phi}_{\text{a}}$ the active DOFs of $\boldsymbol{\Phi}_n$; $\boldsymbol{\Phi}_{\text{a}}^{\text{g}}$ is the generalized inverse of $\boldsymbol{\Phi}_a$. In most cases, the number of measurement points is generally greater than the number of modes in the experimental modal data base. For this case, the generalized inverse can be written as

$$\boldsymbol{\Phi}_{\text{a}}^{\text{g}} = \left(\boldsymbol{\Phi}_{\text{a}}^{\text{T}} \boldsymbol{\Phi}_{\text{a}}\right)^{-1} \boldsymbol{\Phi}_{\text{a}}^{\text{T}} \tag{25}$$

The reduced mass and stiffness matrices can be written as

$$\boldsymbol{M}_{\text{a}} = \boldsymbol{T}_{\text{SEREP}}^{\text{T}} \boldsymbol{M}_n \boldsymbol{T}_{\text{SEREP}} \tag{26}$$

$$\boldsymbol{K}_{\text{a}} = \boldsymbol{T}_{\text{SEREP}}^{\text{T}} \boldsymbol{K}_n \boldsymbol{T}_{\text{SEREP}} \tag{27}$$

2.3.4. Hybrid reduction

This method combines the accuracy of SEREP with the robustness of the Guyan reduction. The transformation matrix is

$$\boldsymbol{T}_{\text{hybrid}} = \boldsymbol{T}_{\text{static}} + (\boldsymbol{T}_{\text{SEREP}} - \boldsymbol{T}_{\text{static}}) \boldsymbol{P} \tag{28}$$

where

$$\boldsymbol{P} = \boldsymbol{\Phi}_{\text{a}} \boldsymbol{\Phi}_{\text{a}}^{\text{T}} \boldsymbol{T}_{\text{SEREP}}^{\text{T}} \boldsymbol{M}_n \boldsymbol{T}_{\text{SEREP}} \tag{29}$$

The reduced mass and stiffness matrices can be written as

$$\boldsymbol{M}_{\text{a}} = \boldsymbol{T}_{\text{hybrid}}^{\text{T}} \boldsymbol{M}_n \boldsymbol{T}_{\text{hybrid}} \tag{30}$$

$$\boldsymbol{K}_{\text{a}} = \boldsymbol{T}_{\text{hybrid}}^{\text{T}} \boldsymbol{K}_n \boldsymbol{T}_{\text{hybrid}} \tag{31}$$

3. Modal analysis

All case studies use a finite element model of a PCB. The PCB under investigation is made of FR4 with 140 mm in length, 120 mm in width, and 2 mm in thickness. The material property is shown in Table 1. The finite element model of the PCB is developed using ANSYS and shown in Fig. 1, consisting of 168 shell elements and 195 nodes. Each node has 6 DOFs, three translational and three rotational. Using this FEM, a free-free analytical solution is obtained for the first ten flexural modes of the PCB.

The experimental modal test arrangement used in this paper is based upon the concept of ''roving hammer''. In this test, the accelerometer is fixed at a single DOF, and the structure is impacted at as many DOFs as desired to define the mode shapes of the structure. The accelerometer and the instrumented hammer are connected to a multi-channel fast Fourier transform (FFT) analyzer which collects both input and output responses and calculated the FRF. By cycling

Table 1 Material property of PCB.

Object	Mass density (kg/m^3)	Elastic modulus (GPa)			Poisson ratio, μ_{xy}
		E_x	E_y	G_{xy}	
PCB	1778	17	17	3.4	0.12

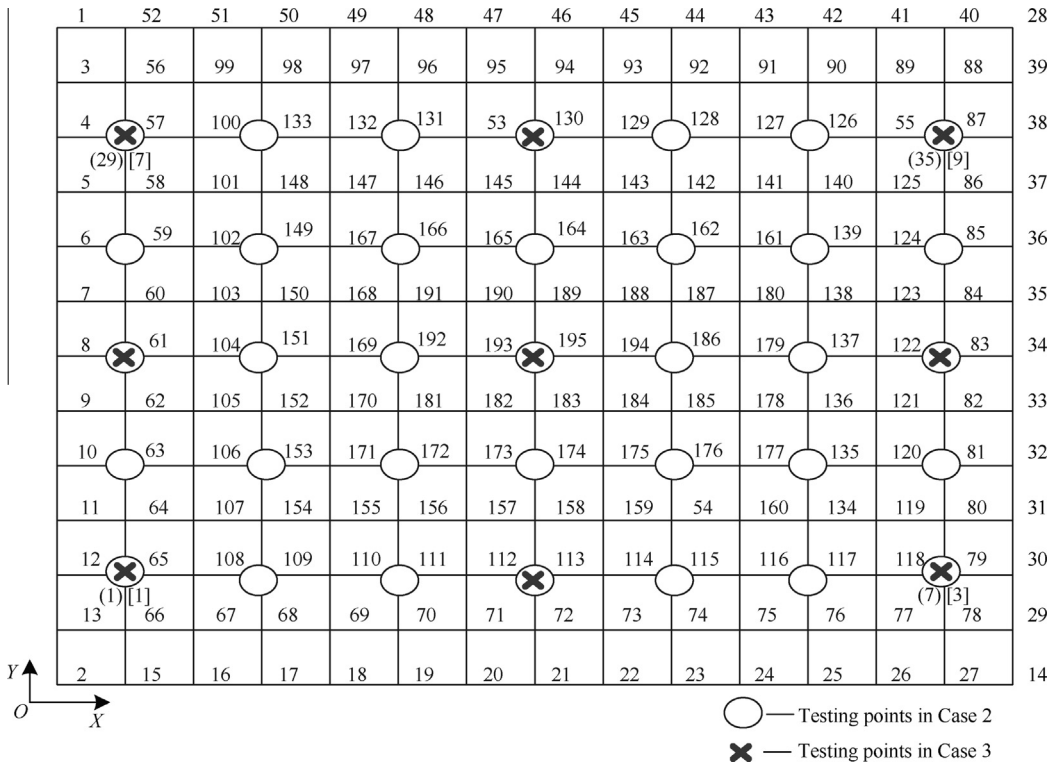

Fig. 1 Finite element model of PCB.

Table 2 First five flexural natural frequencies and mode shapes of modal test and FEM.

Mode No.	Natural frequency (Hz)		Error (%)	Mode shape	
	Modal test	FEM		Modal test	FEM
1	138.21	139.77	1.11	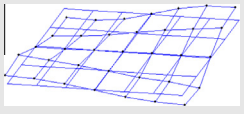	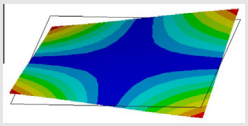
2	258.29	260.44	0.84	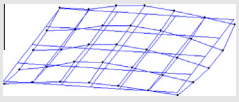	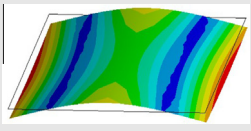
3	352.46	359.49	1.74	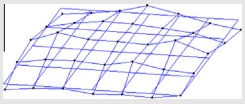	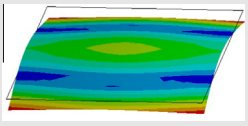
4	392.26	385.58	−1.70	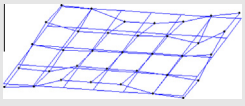	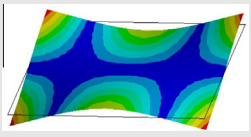
5	456.37	454.63	−0.38	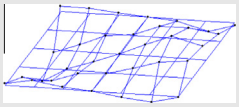	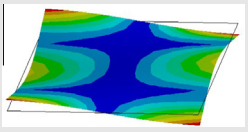

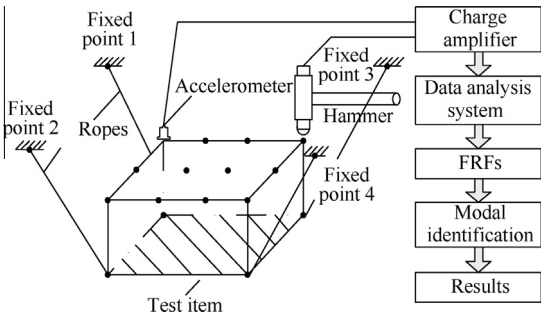

Fig. 2 Modal analysis procedure and instrument.

through all the test points, sufficient frequency response functions are collected to build the transfer matrix and frequency domain global polynomial curve fitting technique (STAR software) is used to estimate the modal parameters. The modal test procedure is shown in Fig. 2. Measurement points are shown by circles and crosses in Fig. 1. Numbers in parenthesis indicate point numbers used in Case 2, and numbers in square brackets indicate point numbers used in Case 3. First five analytical and measured flexural natural frequencies are shown in Table 2. Good correlation is obtained. MAC matrices are shown in case studies.

4. Case studies

Three case studies are presented in this paper. Case 1 demonstrates a new criterion for selecting the best excitation point. Case 2 selects 35 measurement points to perform the modal test and correlation analysis while Case 3 selects 9.

4.1. Case 1—best excitation point

A good excitation point should be able to excite all the modes that are concerned. Assuming only the first ten flexural modes of PCB are considered, the MMP_{qi} for each node is shown in Fig. 3. From Fig. 3 we can see a large difference of excitation effects between different points on different modes. Thus, selection of excitation point need to be based on selected modes. The Minimum MMP_{qi} and MMP_q for each FEM node

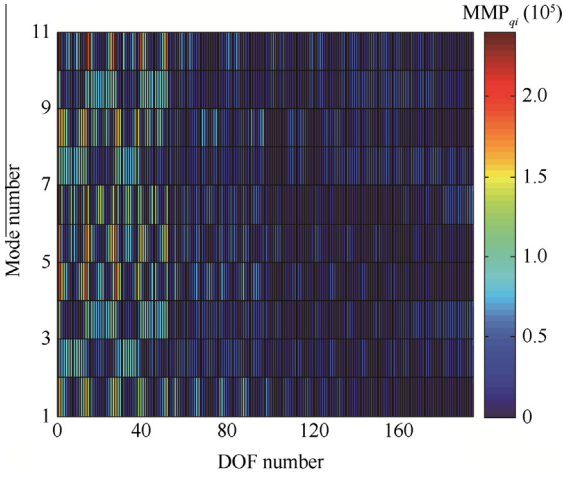

Fig. 3 MMP_{qi} for each node.

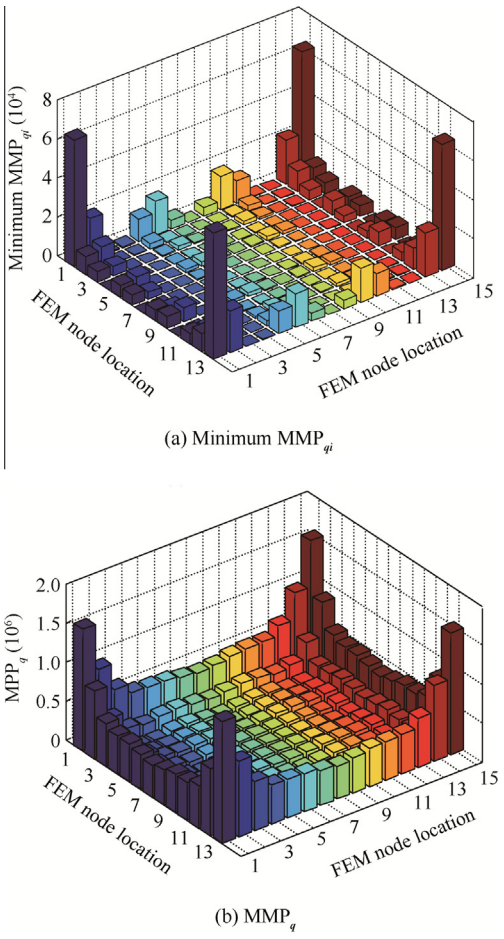

Fig. 4 Minimum MMP_{qi} and MMP_q for each FEM node.

is shown in Fig. 4. From Fig. 4(a) we can see that four corner points have the largest minimum MMP_{qi}. Any one of these points can be selected as the best excitation point. From Fig. 4(b) we can see that the same points have the largest MMP_q. Four best excitation points show up because of the symmetry of PCB and boundary condition.

Although the best excitation points are the same for both criteria, sometimes these points may be inaccessible. The suitability of other nodes as excitation points needs to be evaluated. From Fig. 4(b) we can see that Points (9, 1) and (10, 1) have almost the same MMP_q, which means selecting either one makes no difference. However, we can see from Fig. 4(a) that Point (10, 1) has an MMP_{qi} near zero, which means this point cannot excite at least one of the first ten modes. The drive point mobility for both points are calculated and shown in Fig. 5. As we can see, Point (10, 1) cannot excite mode 3 and 6, which makes it unsuitable as an excitation point when mode 3 and/or 6 are of concern. In contrast, Point (9, 1) can excite all modes. This means the new presented criterion is better than the old one.

4.2. Case 2—35 master DOF

In our experimental modal test, however, these corner points are not used because of their inconvenience for installing the accelerometer. Testing points are shown in Fig. 1. The Minimum MMP_{qi} for each experimental (EXP) node is shown in

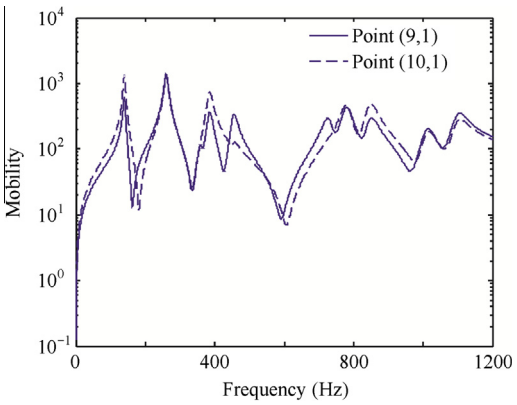

Fig. 5 Drive point mobility for two points.

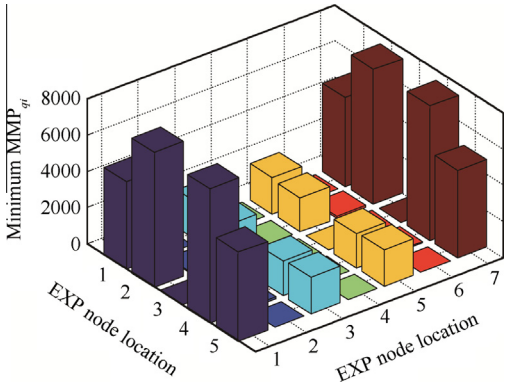

Fig. 6 Minimum MMP_{qi} for each EXP node.

Table 3 MAC for the first five flexural test modes.

Mode No.	1	2	3	4	5
1	1.00	0.02	0.01	0.01	0
2	0.02	1.00	0.03	0.04	0
3	0.01	0.03	1.00	0.03	0
4	0.01	0.04	0.03	1.00	0.03
5	0	0	0	0.03	1.00

Fig. 6. From Fig. 6 we can see that Points 8, 14, 22 and 28 have the largest minimum MMP_{qi}. Point 28 is selected to be the best excitation point. MAC is calculated using the first five flexural test modes and shown in Table 3. Table 3 shows that all diagonal terms are 1 and the off-diagonal terms are close to 0.

Correlation analysis is performed at the reduced DOF. MAC is calculated using the first five flexural analytical and measured modes and shown in Table 4. From Table 4 we can see that good correlation is obtained. The diagonal terms are greater than 0.8 except the fourth mode pair, and the off-diagonal terms are close to 0. The bad correlation between the fourth mode pair may be caused by insufficient test points, bad test points or independence of these two modes. To find out the reason of this bad correlation, POC is calculated and shown in Table 5. From Table 5 we can see that POC (4, 4)

Table 4 MAC for the first five flexural test modes and the corresponding FEM modes (35 DOF).

Mode No.	Test 1	Test 2	Test 3	Test 4	Test 5
FEM 1	0.93	0.02	0	0.01	0
FEM 2	0	0.82	0.03	0	0.01
FEM 3	0	0	0.88	0	0
FEM 4	0	0.01	0.02	0.73	0.01
FEM 5	0	0.01	0	0	0.86

Table 5 POC for the first five flexural test modes and the corresponding FEM modes (35 DOF).

Mode No.	FEM 1	FEM 2	FEM 3	FEM 4	FEM 5
Test 1	1.00	0.01	0	0.01	−0.03
Test 2	0.18	0.98	−0.13	0.15	0.16
Test 3	0.06	0.10	0.98	0.16	0.06
Test 4	0.12	0	−0.07	0.99	−0.02
Test 5	−0.03	−0.04	0.04	−0.10	0.98

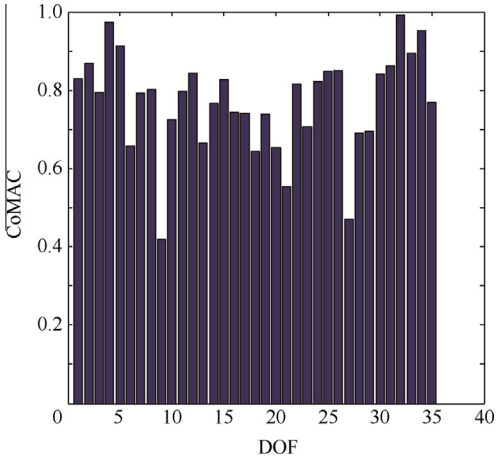

Fig. 7 CoMAC of each DOF.

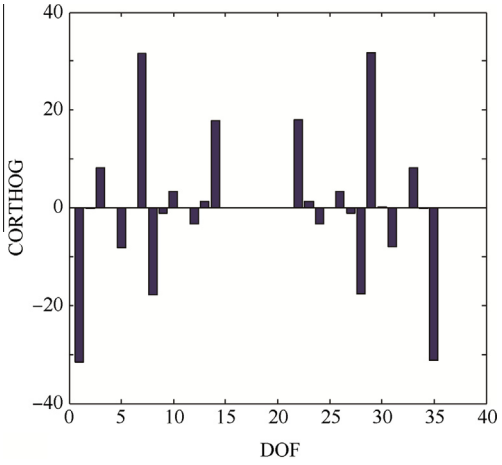

Fig. 8 CORTHOG for each EXP point.

is 0.99, which means the fourth mode pair is the same mode and the bad correlation is caused by insufficient test points.

CoMAC is calculated for each DOF using the first five flexural modes and shown in Fig. 7. Form Fig. 7 we can see which points are badly correlated, i.e., Points 9 and 27. Since the FEM of PCB is very simple, this bad correlation comes from poorly measured data of these bad correlated points. Improvement of test data quality is needed. From Table 5 we can see that all diagonal terms are close to 1, but the (2, 1) term is relatively large compared with 0. In order to identify how each individual DOF contributes to this POC terms, CORTHOG is calculated and shown in Fig. 8. The FEM mass and stiffness matrices are reduced to the 35 DOF using the SEREP reduction methods. The reduced mass matrix (consistent mass matrix) is shown in Fig. 9.

From Fig. 8 we can see that Points 1, 7, 8, 14, 22, 28, 29 and 35 have the largest CORTHOG value. These points are either corner points or near corner points. Since these CORTHOG values are calculated for POC (2, 1), some errors are included either in the second test mode shape or in the first analytical mode shape. As we can see from Table 2, the second experimental mode shape is obviously different from the second analytical mode shape at those points mentioned above, which means there are measurement errors in the modal test. Thus, some additional errors which cannot be identified by using CoMAC can be found by using CORTHOG.

The first TAM is designed to have sufficient DOF to enable the Guyan reduction method to accurately predict the FEM frequencies. The Guyan TAM predicted the FEM frequencies within 3 percent error. The IRS TAM predicted the FEM frequencies exactly. As expected, the SEREP and Hybrid TAMs predicted the frequencies exactly. These results are summarized in Table 6.

Except for the accuracy, the robustness of the 35 DOF TAM is also checked by orthogonality analysis. The reduced mass matrices are shown in Fig. 9.

The ORTHOG are calculated using the first five experimental modes and shown in Tables 7–10. All diagonal terms are normalized to unit for easier comparison between off-diagonal terms. As we can see from Tables 7–10, none of the 35 DOF TAM's robustness is clearly superior to the others.

4.3. Case 3—9 master DOF

Measurement points are shown in Fig. 1. From Figs. 1 and 6 we can see that Points 1, 3, 7 and 9 have the minimum MMP_{qi}. Point 7 is selected as the excitation point. Correlation analysis is performed at the reduced DOF.

MAC is calculated using the first five flexural analytical and measured modes and shown in Table 11. As we can see from Table 11, good correlation is obtained only between the first mode pair, all other diagonal terms are between 0.7 and 0.8,

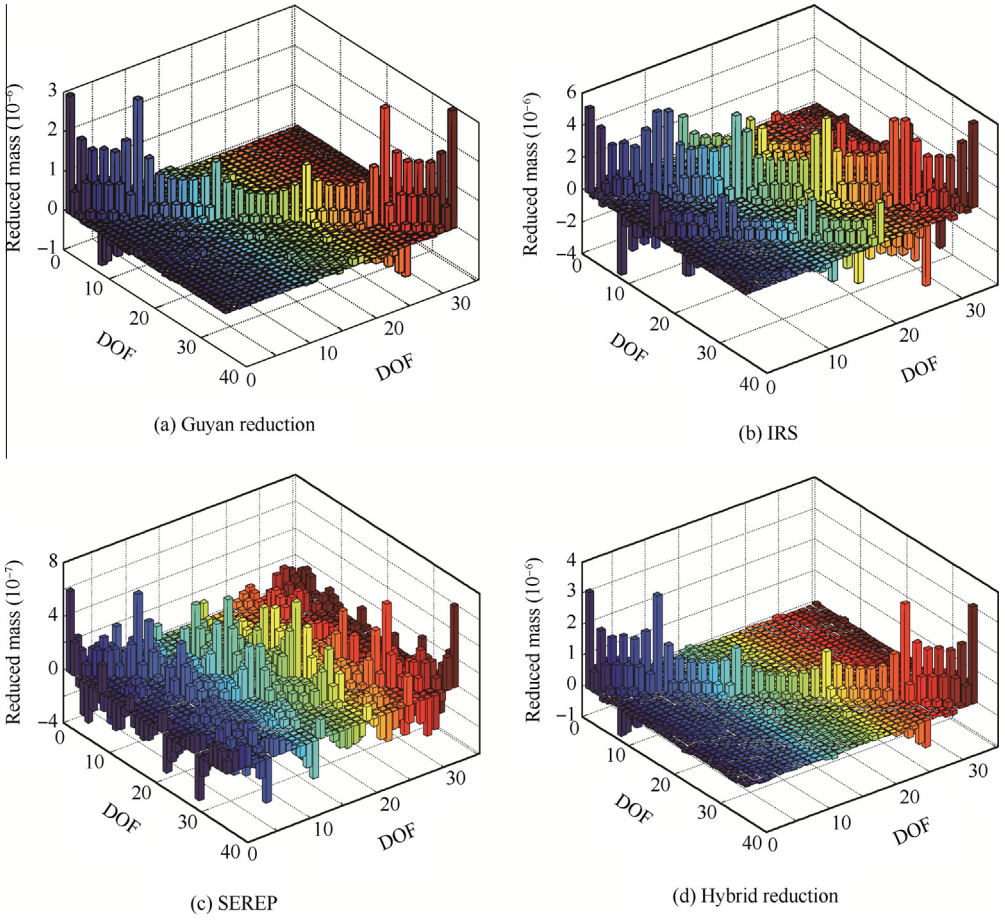

Fig. 9 Reduced mass matrix using four reduction methods.

Table 6 Frequency accuracy for the 35 DOF TAM.

Mode No.	Natural frequency (Hz)	TAM frequency error (%)			
	Original FEM	Guyan	IRS	SEREP	Hybrid
1	139.77	0.3	0	0	0
2	260.44	0.4	0	0	0
3	359.49	2.0	0	0	0
4	385.58	1.6	0	0	0
5	454.63	3.0	0	0	0

Table 7 ORTHOG using Guyan reduction.

Mode No.	1	2	3	4	5
1	1.00	0.14	0.12	0.09	−0.13
2	0.14	1.00	−0.08	0.33	0
3	0.12	−0.08	1.00	−0.04	0
4	0.09	0.33	−0.04	1.00	−0.10
5	−0.13	0	0	−0.10	1.00

Table 8 ORTHOG using IRS.

Mode No.	1	2	3	4	5
1	1.00	0.13	0.14	0.09	−0.19
2	0.13	1.00	−0.15	0.38	0.03
3	0.14	−0.15	1.00	−0.10	−0.10
4	0.09	0.38	−0.10	1.00	−0.08
5	−0.19	0.03	−0.10	−0.08	1.00

Table 9 ORTHOG using SEREP.

Mode No.	1	2	3	4	5
1	1.00	0.19	0.07	0.13	−0.05
2	0.19	1.00	0.02	0.19	0.06
3	0.07	0.02	1.00	0.10	0.09
4	0.13	0.19	0.10	1.00	−0.13
5	−0.05	0.06	0.09	−0.13	1.00

Table 10 ORTHOG using Hybrid reduction.

Mode No.	1	2	3	4	5
1	1.00	0.14	0.12	0.09	−0.13
2	0.14	1.00	−0.10	0.33	0
3	0.12	−0.10	1.00	−0.04	0
4	0.09	0.33	−0.04	1.00	−0.10
5	−0.13	0	0	−0.10	1.00

Table 11 MAC for the first five test modes and FEM modes (9 DOF).

Mode No.	Test 1	Test 2	Test 3	Test 4	Test 5
FEM 1	0.98	0.04	0.02	0.01	0
FEM 2	0	0.74	0.05	0	0.03
FEM 3	0	0	0.77	0.05	0.06
FEM 4	0	0.01	0.15	0.70	0
FEM 5	0	0	0	0.01	0.78

Table 12 POC for the first five test modes and FEM modes (9 DOF).

Mode No.	FEM 1	FEM 2	FEM 3	FEM 4	FEM 5
Test 1	1.00	0.03	0.02	0.05	0
Test 2	0.26	0.98	−0.19	0.13	0.13
Test 3	0.12	0.10	0.95	0.27	0.07
Test 4	0.13	0.09	−0.39	0.89	−0.16
Test 5	−0.06	−0.15	0.33	0	0.93

and the (4, 3) term is obviously larger than that in Table 4 (using 35 master DOF). POC is calculated and shown in Table 12 to show the independence of these modes. Thus, the MAC results indicate that insufficient master DOF leads to bad correlation.

CoMAC is calculated and shown in Fig. 10 to show poorly measured data. From Fig. 10 we can see Point 5 is badly correlated. This bad correlation comes from poorly measured data of these bad correlated points again. Improvement of test data quality is needed. From Table 12 we can see that all diagonal terms are close to 1, but the (4, 3) term is much larger than 0. Comparison is made between Tables 5 and 12, and the results indicate that fewer master DOF tends to degrade the POC. In order to identify how each individual DOF contributes to this POC terms, CORTHOG is calculated and shown in Fig. 11. The FEM mass and stiffness matrices are reduced to the 9 DOF using the SEREP reduction methods. The reduced mass matrix (consistent mass matrix) is shown in Fig. 12.

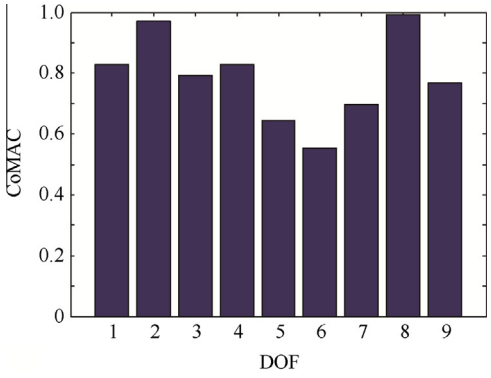

Fig. 10 CoMAC of each DOF.

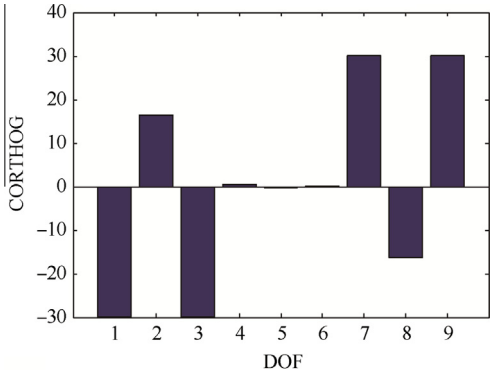

Fig. 11 CORTHOG of each DOF.

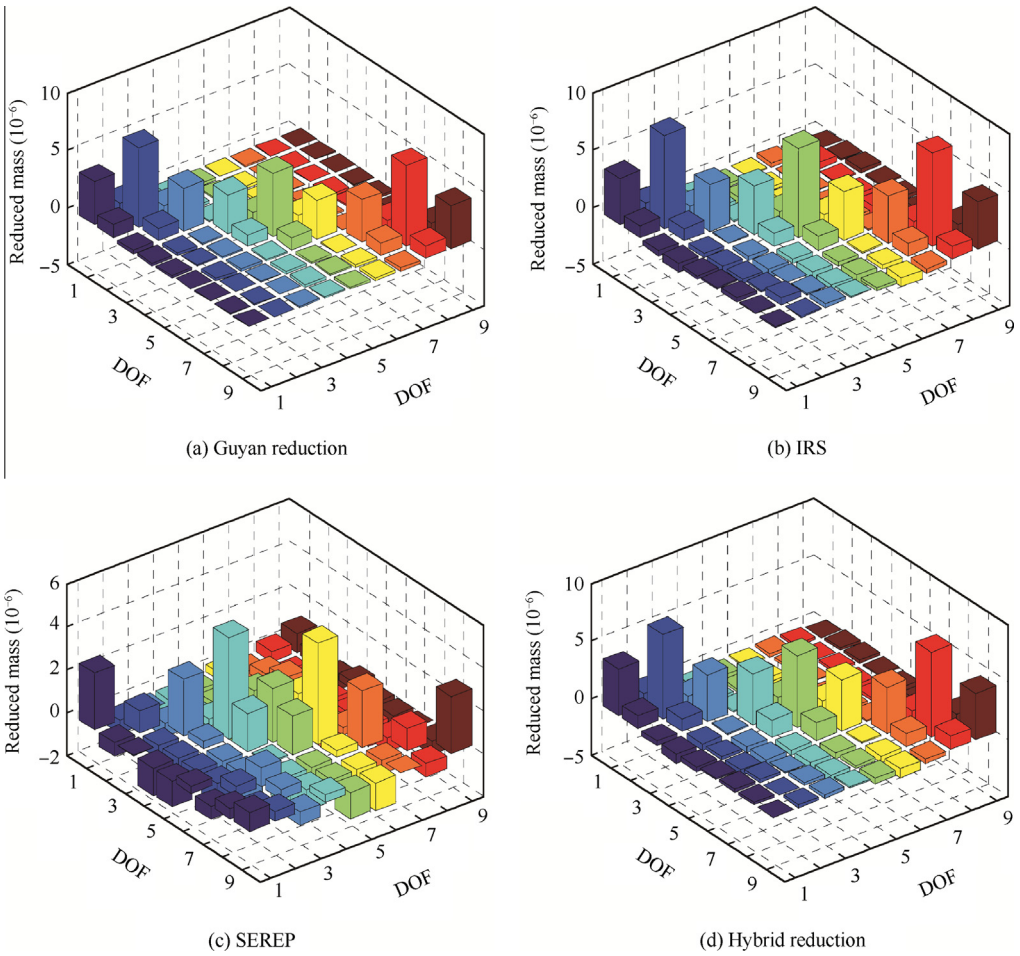

Fig. 12 Reduced mass matrix using four reduction methods.

Table 13 Frequency accuracy for the 9 DOF TAM.

Mode No.	Natural frequency (Hz)	TAM frequency error (%)			
	Original FEM	Guyan	IRS	SEREP	Hybrid
1	139.77	0.9	0	0	0
2	260.44	0.9	0	0	0
3	359.49	8.0	0	0	0
4	385.58	2.5	0	0	0
5	454.63	10.4	0	0	0

From Fig. 11 we can see that Points 1, 3, 7 and 9 have the largest CORTHOG value. These points are all corner points. As explained in Case 1, since these CORTHOG value are also calculated for POC (4, 3), some errors are included in the fourth test mode shape. Thus, some additional errors which are not identified by using CoMAC are found again by using CORTHOG.

POC is calculated using the first five test modes and FEM modes and shown in Table 12.

The second TAM is designed to have insufficient DOF to enable the Guyan reduction method to accurately predict the FEM frequencies. The Guyan TAM predicted the FEM frequencies up to 10.4 percent error. The IRS TAM still predicted the FEM frequencies exactly. As expected, the SEREP and Hybrid TAMs predicted the frequencies exactly. These results are summarized in Table 13.

Table 14 ORTHOG using Guyan reduction.

Mode No.	1	2	3	4	5
1	1.00	0.22	0.16	0.07	−0.05
2	0.22	1.00	0.16	0.46	−0.04
3	0.16	0.16	1.00	0.05	0.30
4	0.07	0.46	0.05	1.00	−0.19
5	−0.05	−0.04	0.30	−0.19	1.00

Table 15 ORTHOG using IRS.

Mode No.	1	2	3	4	5
1	1.00	0.22	0.15	0.07	−0.05
2	0.22	1.00	0.11	0.46	−0.04
3	0.15	0.11	1.00	0	0.29
4	0.07	0.46	0	1.00	−0.21
5	−0.05	−0.04	0.29	−0.21	1.00

The robustness of the 9 DOF TAM is checked by orthogonality analysis. The reduced mass matrices are shown in Fig. 12.

The ORTHOG is calculated using the first three experimental modes and shown in Tables 14–17. All diagonal terms are normalized to unit for easier comparison between off-diagonal terms. As we can see from Tables 14–17, none of the 9 DOF TAM's robustness is clearly superior to the others. However,

Table 16 ORTHOG using SEREP.

Mode No.	1	2	3	4	5
1	1.00	0.29	0.15	0.17	−0.06
2	0.29	1.00	−0.02	0.29	−0.10
3	0.15	−0.02	1.00	−0.11	0.36
4	0.17	0.29	0.11	1.00	−0.30
5	−0.06	−0.10	0.36	−0.30	1.00

Table 17 ORTHOG using Hybrid reduction.

Mode No.	1	2	3	4	5
1	1.00	0.22	0.15	0.07	−0.05
2	0.22	1.00	0.09	0.46	−0.04
3	0.15	0.09	1.00	−0.01	0.31
4	0.07	0.46	−0.01	1.00	−0.22
5	−0.05	−0.04	0.31	−0.22	1.00

the IRS method has a slight improvement over the Guyan reduction and the Hybrid reduction has a slight improvement over the SEREP.

5. Conclusion

(1) The new presented criterion based on MMP can provide more accurate information for selecting the best excitation point than the old criterion does in a modal test.
(2) CORTHOG can be used to find some additional errors which are ignored by CoMAC.
(3) For 35 measurement points, all TAMs predict the first five non-zero FEM frequencies accurately. None of the 35 DOF TAM's robustness is clearly superior to the others.
(4) For 9 testing points, the Guyan TAM predicts the first five non-zero FEM frequencies up to 10.4 percent error. The IRS, SEREP and Hybrid TAMs predict the FEM frequencies exactly. None of the 9 DOF TAM's robustness is clearly superior to the others. However, the IRS method has a slight improvement over the Guyan reduction and the Hybrid reduction has a slight improvement over the SEREP.

Acknowledgement

This study was supported by Science and Technology on Reliability and Environmental Engineering Laboratory, Beihang University. My most sincere appreciation goes to my dear friend, Professor Kjell Ahlin from BTH Sweden. Our long discussions have strongly contributed to this article.

References

1. Pitarresi JM. Modeling of printed circuit cards subject to vibration. In: *Proceedings of the IEEE circuits and systems conference*; 1990. p. 2104–7.
2. Pitarresi JM, Celetka D, Coldwel R, Smith D. The smeared properties approach to FE vibration modeling of printed circuit cards. *J Electron Packag* 1991;**113**(3):250–7.
3. Pitarresi JM, Primavera AA. Comparison of modeling techniques for the vibration analysis of printed circuit cards. *J Electron Packag* 1992;**114**(4):378–83.
4. Lim G, Ong J, Penny J. Effect of edge and internal point support of a printed circuit board under vibration. *J Electron Packag* 1999;**121**(2):122–6.
5. Amy RA, Aglietti GS, Richardson G. Sensitivity analysis of simplified printed circuit board finite element models. *Microelectron Reliab* 2009;**49**(7):791–9.
6. Amy RA, Aglietti GS, Richardson G. Accuracy of simplified printed circuit board finite element models. *Microelectron Reliab* 2010;**50**(1):86–97.
7. Li DS, Li HN, Fritzen CP. The connection between effective independence and modal kinetic energy methods for sensor placement. *J Sound Vib* 2007;**305**(4):945–55.
8. Debnath N, Dutta A, Deb SK. Placement of sensors in operational modal analysis for truss bridges. *Mech Sys Signal Process* 2012;**31**:196–216.
9. Li DS, Fritzen CP, Li HN. Extended MinMAC algorithm and comparison of sensor placement methods. In: *Proceedings of the IMAC-XXVI*; 2008.
10. Ward H. *Modal analysis theory and testing*. 2nd ed. Letchworth: Katholieke Univ. Leuven, Departement Werktuigkunde Press; 1998. p. 75–6.
11. Guyan RJ. Reduction of stiffness and mass matrices. *AIAA J* 1965;**3**(2):380.
12. O'Callahan JC. A procedure for an improved reduced system (IRS) model. In: *Proceedings of the 7th international modal analysis conference*; 1989. p. 17–21.
13. O'Callahan JC, Avitabile P, Riemer R. System equivalent reduction expansion process (SEREP). In: *Proceedings of the 7th international modal analysis conference*; 1989. p. 29–37.
14. Sairajan KK. Robustness of system equivalent reduction expansion process on spacecraft structure model validation. *AIAA J* 2012;**50**(11):2376–88.
15. Kammer D. A hybrid approach to test-analysis model development for large space structures. *J Vib Acoust* 1991;**113**(3):325–32.
16. Nimityongskul S, Kammer DC. Frequency domain model reduction based on principal component analysis. *Mech Sys Signal Process* 2010;**24**(1):41–51.
17. Koutsovasilis P. Comparison of model reduction techniques for large mechanical systems. *Multibody Sys Dyn* 2008;**20**(2):111–28.
18. Zang C, Grafe H, Imregun M. Frequency–domain criteria for correlating and updating dynamic finite element models. *Mech Sys Signal Process* 2001;**15**(1):139–55.
19. Pradhan S, Modak SV. Normal response function method for mass and stiffness matrix updating using complex FRFs. *Mech Sys Signal Process* 2012;**2012**(32):232–50.
20. Sipple JD, Sanayei M. Finite element model updating using frequency response functions and numerical sensitivities. *Struct Control Health Monit* 2013;**21**(5):784–802.
21. Allemang RJ. The modal assurance criterion—twenty years of use and abuse. *Sound Vib* 2003;**37**(8):14–21.
22. Peeters B, Ventura CE. Comparative study of modal analysis techniques for bridge dynamic characteristics. *Mech Sys Signal Process* 2003;**17**(5):965–88.
23. Zárate BA, Caicedo JM. Finite element model updating: multiple alternatives. *Eng Struct* 2008;**30**(12):3724–30.

Xu Fei is a Ph.D. student at School of Reliability and System Engineering, Beihang University. He received his B.S. degree from Nanjing University of Aeronautics and Astronautics in 2009. His area of research includes structural dynamics, shock and vibration, modal analysis, finite element analysis, fatigue analysis, etc.

Li Chuanri is a professor at School of Reliability and Systems Engineering, Beihang University. He is a member of IEC TC104 MT17. His main research interests are environmental engineering, shock and vibration, reliability test etc.